Experimental demonstration of selective compression of femtosecond pulses in the Laue scheme of the dynamical Bragg diffraction in 1D photonic crystals

S. E. Svyakhovskiy,[1,*] A. A. Skorynin,[1] V. A. Bushuev,[1] S. V. Chekalin,[2] V. O. Kompanets,[2] A. I. Maydykovskiy,[1] T. V. Murzina,[1] and B. I. Mantsyzov[1]

[1]*Department of Physics, M. V. Lomonosov Moscow State University, Moscow, 119992, Russia*
[2]*Institute for Spectroscopy RAS, Troitsk, Moscow Region, 142190, Russia*

[*]*sse@shg.ru*

Abstract: We present the experimental results of diffraction-induced temporal splitting of chirped femtosecond optical pulses under the dynamical Bragg diffraction in the Laue geometry. For the experiments we made a transparent, high quality porous-quartz based 1D photonic crystal composed of 500 layers. We demonstrate that a selective compression of pulses is observed in this case, that is only one pulse from the pair is compressed, while the second one is broadened. This selective compression effect is determined by the sign and the value of the chirp parameter of the input pulse, in agreement with the theoretical description.

OCIS codes: (050.1940) Diffraction; (320.5540) Pulse shaping; (050.5298) Photonic crystals; (350.4238) Nanophotonics and photonic crystals.

References and links

1. P. St. J. Russell, "Bragg resonance of light in optical superlattices," Phys. Rev. Lett. **56**(6), 596–599 (1986).
2. P. St. J. Russell, "Optical superlattices for modulation and deflection of light," J. Appl. Phys. **59**(10), 3344–3355 (1986).
3. V. G. Baryshevsky and S. A. Maksimenko, "Light pulse dispersion under Laue diffraction from a spatial holographic grating," Opt. Commun. **94**, 379 (1992).
4. B. I. Mantsyzov, "Laue soliton in resonantly absorbing photonic crystal," Opt. Commun. **189**, 275–280 (2001).
5. D. Mandelik, H. S. Eisenberg, Y. Silberberg, R. Morandotti, and J. S. Aitchison, "Band-gap structures of waveguide arrays and excitation of Floquet-Bloch solitons," Phys. Rev. Lett. **90**(5), 053902 (2003).
6. M. Calvo, P. Cheben, O. Martinez-Matos F. del Monte, and J. A. Rodrigo, "Experimental detection of the optical Pendellösung efect," Phys. Rev. Lett. **97**, 084801 (2006).
7. S. Savo, E. Di Gennaro, C. Miletto, A. Andreone, P. Dardano, L. Moretti, and V. Mocella, "Pendellösung effect in photonic crystals," Opt. Express **16**, 9097–9105 (2008).
8. V. A. Bushuev, B. I. Mantsyzov, and A. A. Skorynin, "Diffraction-induced laser pulse splitting in a linear photonic crystal," Phys. Rev. A **79**, 053811 (2009).
9. S. E. Svyakhovskiy, V. O. Kompanets, A. I. Maidykovskiy, T. V. Murzina, S. V. Chekalin, V. A. Bushuev, A. A. Skorynin, and B. I. Mantsyzov, "Observation of diffraction-induced laser pulse splitting in a photonic crystal," Phys. Rev. A **86** 013843 (2012).
10. A. A. Skorynin, V. A. Bushuev, and B. I. Mantsyzov, "Dynamical Bragg diffraction of optical pulses in photonic crystals in the Laue geometry: diffraction-induced splitting, selective compression, and focusing of pulses," J. Experim. Theor. Phys. **115**, 56–67 (2012).
11. S. E. Svyakhovskiy, A. A. Skorynin, V. A. Bushuev, S. V. Chekalin, V. O. Kompanets, A. I. Maydykovskiy, T. V. Murzina, V. B. Novikov, and B. I. Mantsyzov, "Polarization effects in diffraction-induced laser pulse splitting in one-dimensional photonic crystals," J. Opt. Soc. Am. B **30**(5), 1261–1269 (2013).

#224414 - $15.00 USD Received 6 Oct 2014; revised 23 Nov 2014; accepted 26 Nov 2014; published 5 Dec 2014

12. B. Bruser, I. Staude, G. Freymann, M. Wegener, and U. Pietsch, "Visible light Laue diffraction from woodpile photonic crystals," Appl. Opt. **51**, 6732–6737 (2012).
13. L. Maigyte, T. Gertus, M. Peckus, J. Trull, C. Cojocaru, V. Sirutkaitis, and K. Staliunas, "Signatures of light-beam spatial filtering in a three-dimensional photonic crystal," Phys. Rev. A **82**, 043819 (2010).
14. B. Terhalle, A. Desyatnikov, D. Neshev, W. Krolikowski, C. Denz, and Y. S. Kivshar, "Dynamic diffraction and interband transition in two-dimensional photonic lattices," Phys. Rev. Lett. **106**, 083902 (2011).
15. R. W. James, *Optical Principles of the Diffraction of X-Rays* (Cornell University Press, 1965).
16. Z. G. Pinsker, *Dynamical Scattering of X-rays in Crystals*, Springer Ser. Solid-State Sci., Vol. 3 (Springer, 1977).
17. G. Borrmann, "Über Extinktionsdiagramme der Röntgenstrahlen von Quarz," Physik. Z. **42** 157 (1941).
18. S. E. Svyakhovskiy, A. I. Maydykovskiy, and T. V. Murzina, "Mesoporous silicon photonic structures with thousands of periods," J. Appl. Phys. **112**(1), 013106 (2012).
19. S. A. Akhmanov, V. A. Vysloukh, and A. S. Chirkin, *Optics of Femtosecond Laser Pulses* (AIP, 1992).
20. A. Taflove, S. Hagness, *Computational Electrodynamics: The Finite-Difference Time-Domain Method*, 3rd ed. (Artech House, 2005).

1. Introduction

Optical effects accompanying the dynamical Bragg diffraction in photonic crystals (PC) [1–6] are being intensively studied in the last years [7–14]. This high activity is in part due to a significant progress in modern technologies, which allows to fabricate high-quality PC structures. The dynamical diffraction means the energy exchange between the transmitted and diffracted waves during their propagation within a PC and can be observed only in diffraction-thick photonic crystals made of several hundreds of layers. The interest to the effects accompanying the dynamical Bragg diffraction is caused by new perspectives in their applications for controlling the parameters and dynamics of optical pulses.

Following the formalism of the X-ray optics, the boundary problem of the Bragg diffraction in a PC can be divided into two groups, which correspond to the Bragg geometry (in reflection) or to the Laue one (in transmission) [15, 16]. In the first case the total Bragg reflection at the PC boundary can be realized leading to the formation of the photonic band gap. On the contrary, strongly coupled waves that propagate within a PC in the Laue diffraction scheme (Fig. 1(a)) do not experience strong losses under the reflection from the interfaces within a PC structure. In that case, a number of strongly interacting waves is determined by the number of nodes of the reciprocal lattice within the Ewald sphere [15].

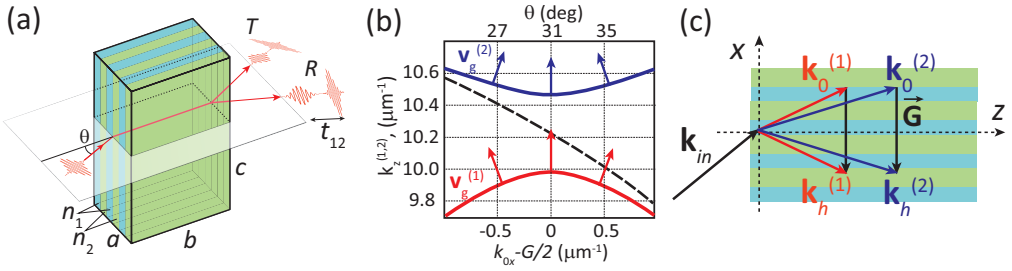

Fig. 1. (a) Schematic diagram of time splitting of chirped incident pulse within 1D PC in the Laue geometry; T and R are the transmitted and diffractively reflected pairs of pulses; t_{12} is the time delay between the splitted pulses. (b) Isofrequency curves for the Borrmann (red line) and anti-Borrmann (blue line) modes close to the Bragg diffraction condition $k_{0x} = G/2$; θ is the angle of incidence of the input radiation; group velocities $\mathbf{v}_g^{(1)}$, $\mathbf{v}_g^{(2)}$ are shown by arrows. Dashed line corresponds to the dispersion curve of the effective medium. (c) Vector diagram shows the wave vectors $\mathbf{k}_{0,h}^{(1,2)}$ of the four interacting waves propagating in a PC, $\mathbf{G}$ is the reciprocal lattice vector.

Isofrequency dispersion curves $\omega(k_{ox}, k_z) = const$ (Fig. 1(b)) are commonly used for the

#224414 - $15.00 USD Received 6 Oct 2014; revised 23 Nov 2014; accepted 26 Nov 2014; published 5 Dec 2014

analysis of the dynamical diffraction of waves transmitted through a PC [8, 10, 11]. The diffracted waves with $k_{hx} = k_{0x} - G$ are described by similar symmetric curves, where G is the absolute value of the reciprocal lattice vector. It is clear from Fig. 1 that four waves propagate in a PC for the case of the Laue diffraction scheme. The two waves with the wave vectors $\mathbf{k}_0^{(1,2)} = (k_z^{(1,2)}; k_{0x})$ propagate in the direct direction and the two waves with $\mathbf{k}_h^{(1,2)} = (k_z^{(1,2)}; k_{hx} = k_{0x} - G)$ correspond to the diffracted direction, as is shown in Fig. 1(c). Importantly that the tangential wave vector components of the direct waves k_{0x} are equal to each other and real, as they are determined by the boundary condition $k_{0x} = k_{inx}$, where k_{inx} is the x-projection of the wave vector of the incident wave, $\mathbf{k}_{in}$. The $z-$components of the wave vectors $k_z^{(1,2)}$ are real quantities as well, which means that the waves propagate within a PC in the Laue scheme without losses for any frequency ω and at any angle of incidence θ. In other words, no photonic band gap appears for both longitudinal and transversal propagation directions even for an exact fulfilment of the "transversal" Bragg diffraction condition.

These four waves in pairs form the two propagating modes, Borrmann and anti-Borrmann ones [15–17]. The first one is formed by the direct and diffracted waves with smaller values of the wave vector projection $k_z = k_z^{(1)}$. Such waves propagate with the same group velocity $\mathbf{v}_g^{(1)}$ along the normal to the corresponding dispersion curve (see Fig. 1(b)) and are spatially localized in the layers with smaller refractive index. The second, anti-Borrmann, mode is localized in the layers with higher refractive index and is formed by the waves with larger $k_z = k_z^{(2)}$ values. Their group velocity $\mathbf{v}_g^{(2)}$ coincides with $\mathbf{v}_g^{(1)}$ only under the exact fulfilment of the Bragg diffraction condition. Amplitudes of both Borrmann and anti-Borrmann waves are determined by their deviation from the Bragg condition [11]. If all four waves are present in the same point of a PC, their interference results in a periodic swap of energy from the directly propagating wave to the diffracted one and vice versa, which appears as the so called Pendellösung effect [6–9, 15, 16]. It is of high interest for all-optical switching of light in photonic crystals.

During their propagation in a PC, Borrmann and anti-Borrmann light pulses split temporally due to their different spatial localization (different group velocity $\mathbf{v}_g^{(1)}$ and $\mathbf{v}_g^{(2)}$) (Fig. 1(b)). This allows for the temporal diffraction-induced splitting of short laser pulses for a sufficient size of the PC [8–11]. Outside the PC each of the two pulses splits spatially into two ones, which correspond to the direct and diffracted directions, as is shown in Fig.1(a). This is due to the breakdown of tight bonding of direct and diffracted waves outside the PC. Besides, it was shown that the dispersion of transversal projections of the group velocities of the Borrmann and anti-Borrmann pulses, $v_{gx}^{(1)}$ and $v_{gx}^{(2)}$, are different in sign [10]. Thus it was proposed that a selective compression can take place for *chirped* pulses propagating within a PC, which consists in a compression of one of the outgoing pulses and broadening of the other one depending on the chirp sign. To the best of our knowledge, up to now there have been no experimental verifications of this effect.

In this paper we show the first experimental evidence of the existence of *selective* compression of chirped femtosecond laser pulses in 1D PC in the Laue diffraction scheme. We demonstrate experimentally that for the case of porous quartz based PC, either the Borrmann or the anti-Borrmann pulses are compressed depending on the sign of the chirp parameter. The experimental results are in a good agreement with the finite-difference time-domain (FDTD) numerical modelling and with the analytical description [10].

2. Experimental samples and setup

The experiments were performed for 1D photonic crystal composed of porous fused silica layers of different porosity made by the procedure described in detail elsewhere [18]. 1D porous

#224414 - $15.00 USD Received 6 Oct 2014; revised 23 Nov 2014; accepted 26 Nov 2014; published 5 Dec 2014

silicon PC was made by electrochemical etching of crystalline Si(001) of the resistivity of 0.001 $\Omega\times$cm in a 28% water-ethanol HF solution. Periodic modulation of porosity was attained by using the periodically alternating etching current of 40 mA/cm^2 and 200 mA/cm^2, thus a periodical modulation of the refractive index of porous silicon in the direction normal to Si(001) surface was achieved. Using this procedure, a PC consisting of 250 pairs of layers was made. After that it was thermally annealed for 4 hours at the temperature of 850°C until the total oxidation of silicon thus forming a 1D PC. The refractive indices of alternating porous fused silica layers were $n_1 = 1.43 \pm 0.01$ and $n_2 = 1.32 \pm 0.01$, the period of the structure is 825 nm, the size of the sample being $a = 0.2$ mm, $b = 2.3$ mm, $c \approx 5$ mm (Fig. 1(a)).

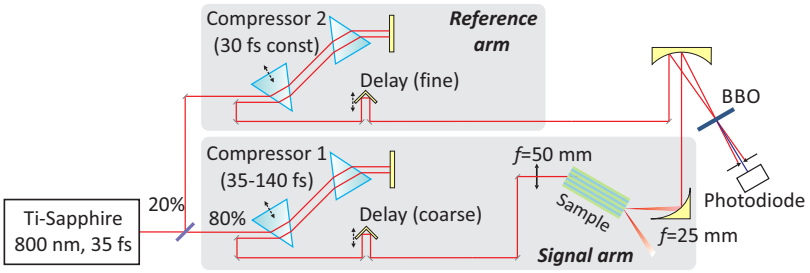

Fig. 2. Schematic view of the experimental setup.

The experimental set-up is shown schematically in Fig. 2. Linearly-polarized radiation of a Ti-sapphire laser operating at 800 nm wavelength with the pulse duration of 35 fs and repetition rate of 80 MHz, average power up to 400 mW was used as the fundamental radiation. A cross-correlation scheme with the signal and the reference arms containing prism compressors was used. The compressor in the reference arm was fixed to maintain 30 fs reference pulses, while the compressor in the signal arm could be tuned and formed the chirped pulses with the duration from 35 fs up to 140-150 fs for the negative (low frequency first) and the positive (high frequency first) chirp. A linearly chirped pulse can be characterized by the dimensionless chirp parameter β [10] given by $\beta = \pm\sqrt{(\tau/\tau_0)^2 - 1}$ [19], where τ_0, τ are the measured full width at half magnitude (FWHM) of the initial and output chirped pulses duration, $\pm$ is the chirp sign. In these terms, the β values available experimentally range from -4.5 to $+4.0$. After passing through a compressor, the laser beam was focused on the facet of the sample into a spot of 20 μm in diameter by a lens with $f = 50$ mm.

The output beam was gathered by a 25 mm parabolic mirror and focused on a nonlinear BBO crystal along with the reference beam (Fig. 2, right). The second harmonic signal generated in a non-collinear geometry was detected by an avalanche photodiode, which allowed to measure the *cross-correlation* function $I_{CC}(t') \propto \int_{-\infty}^{\infty} I_S(t) I_R(t+t')dt$, where $I_S(t)$ and $I_R(t)$ are the intensities in the signal and reference channels, t' is the delay time between them. In case of Gaussian pulses, the FWHM of the cross-correlation function τ_{CC} depends on FWHMs of the signal pulse τ_S and of the reference pulse τ_R as $\tau_{CC}^2 = \tau_S^2 + \tau_R^2$. For the constant reference pulse width of 30 fs, the τ_S can be reconstructed from the τ_{CC} allowing to study the selective compression of short chirped pulses. The temporal resolution of the set-up evaluated in test measurements was $\approx$2 fs. The temporal delay between the Borrmann and anti-Borrman pulses remains constant as there are no dispersion elements between the sample and the BBO crystal.

3. Experimental Results and Discussion

Figure 3 shows the experimental data on cross-correlation functions measured for the values of the chirp factor $\beta = -2.2, -0.1, +1.6$. It can be seen that I_{CC} shown by black line consists

#224414 - $15.00 USD Received 6 Oct 2014; revised 23 Nov 2014; accepted 26 Nov 2014; published 5 Dec 2014

of two maxima, which corresponds to the two temporally split pulses, the Borrmann and the anti-Borrmann. The cross-correlation function maximum centered at approximately −400 fs corresponds to the faster Borrmann pulse, while the second peak at 350 fs stands for the anti-Borrmann one. For comparison, cross-correlation functions of the incident pulse measured on the same set-up by removing the sample from the optical path are shown in the same panels.

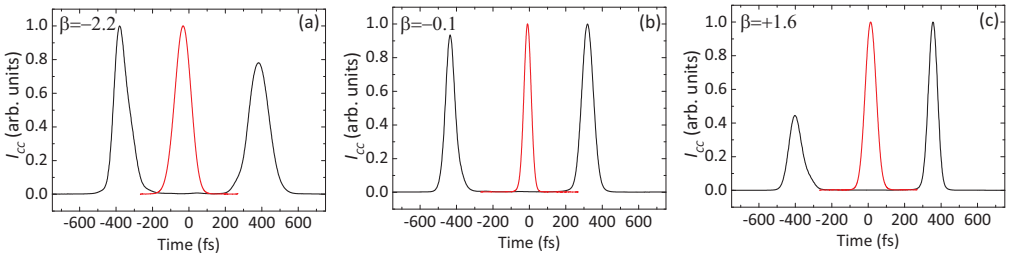

Fig. 3. Cross-correlation functions (black line) of pulses after passing through the PC for the incident pulse chirp parameter (a) $\beta = -2.2$, (b) $\beta = -0.1$ and (c) $\beta = +1.6$; central (red line) pulse corresponds to the laser pulse before entering the PC.

It stems from Fig. 3(b) that for almost zero chirp parameter of the incident pulse $\beta = -0.1$ the durations of the two output pulses are almost equal. Note that signs of the output pulses chirps are different. For the positive chirp $\beta = 1.6$ the width of the Borrmann pulse is approximately $\tau_B = 87$ fs, which is significantly larger than that of the anti-Borrmann one $\tau_{aB} = 53$ fs and incident pulse of $\tau = 70$ fs. For the negative chirp $\beta = -2.2$ a controversial effect occurs: the anti-Borrmann pulse broadens up to $\tau_{aB} = 125$ fs, and the Borrmann pulse undergoes compression up to $\tau_B = 75$ fs in comparison with the initial pulse $\tau = 89$ fs.

Dependencies of the Borrmann and anti-Borrmann pulsewidths on the chirp factor were measured for β ranging from -4 to $+4$. The corresponding dependences are shown in Fig. 4(a) in comparison with the pulsewidth τ of the input pulse. It can be seen that the the pulsewidth of the Borrmann pulse exceeds that of the anti-Borrmann one in the case of $p-$polarization of the input radiation, while for positive β values and for $\beta > +1$ its width is larger than of the incident pulse. For negative β values the situation is reversed: the Borrmann pulse is compressed as compared to the anti-Borrmann one and for $\beta < -1.5$ its pulsewidth is also smaller than that of the incident pulse. In other words, the effect of selective compression is observed, which manifests itself by the shortening of the anti-Borrmann (Borrmann) pulses for the positive (negative) β values.

This result is in a qualitative agreement with the analytical theory based on the two-wave approximation [10]. At the same time, this approximation is valid for the *quantitative* description of the pulse propagation only in the case of a relatively narrow spectrum ($\tau > 60$ fs for non-chirped pulse). Therefore we used a numerical simulation (FDTD) for the quantitative description of the effect as in our experiment the laser pulses are about 30 fs in duration.

The simulation of the selective compression effect was performed using FDTD method and our own code based on [20]. Figure 4(b) shows the corresponding FDTD results calculated for the parameters realized in the experiments in case of $p-$polarization of the incident pulse. The compression of the anti-Borrmann pulse occurs at $\beta > +1$ and the compression of the Borrmann pulse takes place for $\beta < -1$, which correlates with the experiment. Figure 4(c) shows the comparison of the measured intensity of the pulse with $\beta = -2.2$ passed from the crystal (black line) and the calculated one, which shows an excellent quantitative agreement of the theory and the experimental results. The effect of selective compression of the chirped laser pulses is observed also for the $s-$polarized fundamental pulsed radiation, as is shown in Fig.

#224414 - $15.00 USD Received 6 Oct 2014; revised 23 Nov 2014; accepted 26 Nov 2014; published 5 Dec 2014

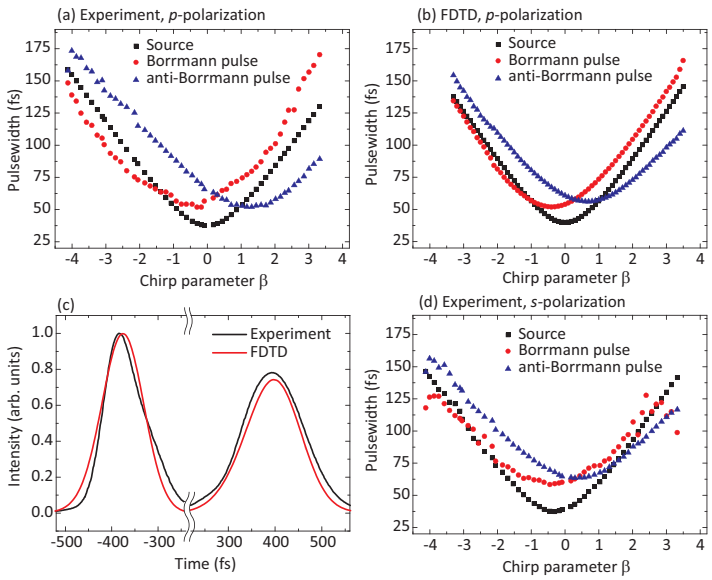

Fig. 4. (a) Experimental and (b) theoretical dependencies of the Borrmann and anti-Borrmann pulsewidths on the chirp β of the incident pulse in comparison with the initial pulsewidth for $p-$polarization of incident pulse. (c) Experimental (black line) and theoretical (red line) temporal functions of the pulse intensity for $\beta = -2.2$. (d) Experimental dependence of Borrmann and anti-Borrmann pulsewidths on the chirp of incident pulse in comparison with the initial pulsewidth for $s-$polarization of incident pulse.

4(d). The effect is qualitatively similar to the case of p-polarized fundamental radiation, while the modulation of the pulsewidths is smaller. The critical chirp values, which correspond to the equal values of the pulsewidths of the incident and the output pulses, are also higher and are $\beta \gtrsim 1.5$.

4. Conclusion

The temporal Bragg diffraction-induced splitting of femtosecond optical pulses with *frequency modulated phase* under the dynamical Bragg diffraction in the Laue scheme in 1D photonic crystal has been studied experimentally. We demonstrate that depending on the chirp sign, the compression of either Borrmann or anti-Borrmann pulses is attained. This effect of selective compression of the separated chirped pulses was first observed. The experimental results are in good agreement with theoretical prediction [10] and with FDTD numerical simulation carried out here. The selective compression of optical pulses can be used to considerably increase the yield of nonlinear processes (harmonic generation, two-photon absorption, nonlinear phase modulation, etc.) in PCs by increasing the intensity of the Borrmann or anti-Borrmann pulse by more than an order of magnitude if the value of the chirp is large enough. Addition, the parameters (duration, amplitude, phase, etc) of the Borrmann and anti-Borrmann pulses can be controlled independently.

Acknowledgments

This work was partially supported by the Russian Foundation for Basic Research, grants No.13-02-00300, No.14-29-07197 and No.14-02-31770.

#224414 - $15.00 USD Received 6 Oct 2014; revised 23 Nov 2014; accepted 26 Nov 2014; published 5 Dec 2014